

Article

A Novel and Efficient Method for the Synthesis of Methyl (*R*)-10-Hydroxystearate and FAMES from Sewage Scum

Luigi di Bitonto, Valeria D'Ambrosio and Carlo Pastore * 

Water Research Institute (IRSA), National Research Council (CNR), via F. de Blasio 5, 70132 Bari, Italy; luigi.dibitonto@ba.irsa.cnr.it (L.d.B.); valeria.dambrosio@ba.irsa.cnr.it (V.D.)

* Correspondence: carlo.pastore@ba.irsa.cnr.it

Abstract: In this work, the transesterification of methyl estolides (ME) extracted from the lipid component present in the sewage scum was investigated. Methyl 10-(*R*)-hydroxystearate (Me-10-HSA) and Fatty Acid Methyl Esters (FAMES) were obtained in a single step. A three-level and four factorial Box–Behnken experimental design were used to study the effects of methanol amounts, catalyst, temperature, and reaction time on the transesterification reaction using aluminum chloride hexahydrate ($\text{AlCl}_3 \cdot 6\text{H}_2\text{O}$) or hydrochloric acid (HCl) as catalysts. $\text{AlCl}_3 \cdot 6\text{H}_2\text{O}$ was found quite active as well as conventional homogeneous acid catalysts as HCl. In both cases, a complete conversion of ME into Me-10-HSA and FAMES was observed. The products were isolated, quantified, and fully characterized. At the end of the process, Me-10-HSA (32.3%wt) was purified through a chromatographic separation and analyzed by NMR. The high enantiomeric excess ($ee > 92\%$) of the *R*-enantiomer isomer opens a new scenario for the valorization of sewage scum.

Keywords: sewage scum; methyl (*R*)-10-hydroxystearate; FAMES; biodiesel; estolides



Citation: di Bitonto, L.; D'Ambrosio, V.; Pastore, C. A Novel and Efficient Method for the Synthesis of Methyl (*R*)-10-Hydroxystearate and FAMES from Sewage Scum. *Catalysts* **2021**, *11*, 663. <https://doi.org/10.3390/catal11060663>

Academic Editor: Domenico Licursi

Received: 24 April 2021

Accepted: 21 May 2021

Published: 23 May 2021

Publisher's Note: MDPI stays neutral with regard to jurisdictional claims in published maps and institutional affiliations.



Copyright: © 2021 by the authors. Licensee MDPI, Basel, Switzerland. This article is an open access article distributed under the terms and conditions of the Creative Commons Attribution (CC BY) license (<https://creativecommons.org/licenses/by/4.0/>).

1. Introduction

Hydroxy Fatty Acids (HFAs) are valuable raw materials widely used for several industrial applications, including resins, polymers, cosmetics, biofuels, biolubricants, and additives in coatings and paintings [1,2]. They are valuable intermediates for synthesizing chemicals and pharmaceuticals for their antibiotic, anti-inflammatory, and anticancer properties [3,4].

HFAs are ubiquitous as constituents of plants, seeds, insects, animals and other microorganisms [5,6]. Many of these natural sources are found as part of estolides, oligomeric fatty acid esters formed by hydroxy acyl groups bonded together with ester bonds [7]. Estolides are being marketed as biolubricants for automotive and industrial applications for their excellent physicochemical properties as high viscosity and flash point, good resistance and biodegradability [8–10].

Since its first discovery, 10-(*R*)-Hydroxystearic acid (10-HSA) has attracted great industrial interest. It is the natural precursor of γ -(*R*)-dodecalactone, a taste and aroma component used in the flavor and fragrance industry [11–13]. Moreover, it is used in the manufacturing of lubricants and cosmetics for its chemical properties similar to those of Ricinoleic acid (or 12-Hydroxystearic acid) [14,15].

In recent years, different studies have been carried out for the production of 10-HSA, based on the enzymatic hydrolysis of vegetable oils from bacteria and microorganisms, such as *Elizabethkingia meningoseptica* [16], *Enterococcus faecalis* [17], *Lactobacillus plantarum* [18], *Lysinibacillus fusiformis* [19], *Nocardia cholesterolicum* [20], *Selenomonas ruminantium* [21], *Stenotrophomonas nitritireducens* [22], *Stenotrophomonas maltophilia* [23], *Sphingobacterium thalophilum* [24]. Fatty acid hydratases have shown to be efficient catalysts with a good regio- and stereoselectivity, particularly useful to obtaining pure enantiomeric forms [25,26]. However, their applicability is not competitive with the currently existing conventional diesel-producing technology for a series of drawbacks, including (i) the specificity of the

widely adopted in studies concerning the production of biodiesel for optimizing the transesterification reaction [47–50]. Notably, a Box–Behnken factorial design of experiments was used. The amount of methanol and catalyst, temperature and reaction time were optimized with the aim of maximizing the conversion of ME into Me-10-HSA and FAMES.

2. Analysis of Results

2.1. Characterization of the Lipid Component of Sewage Scum and Biodiesel Production

Biofuels are considered the leading renewable energy sources, presenting several advantages with respect to conventional fossil fuels [51,52]. Nevertheless, the high production costs associated with the raw materials (vegetable oils and animal fats) result in a significant increase in their price [42,43].

Sewage scum can be considered a cheap and available feedstock to synthesize biofuels due to its high lipid content (up to 36–50% of dry weight) [29]. The lipid fraction, very rich in FFAs, can be easily converted into FAMES by acid-catalyzed direct esterification [53–55]. However, the high water content in the sewage scum (TS = 10–25%wt) represents a significant obstacle to biodiesel production at a commercial scale. The initial stages, from the collection of the raw sludge to the dehydration and drying, are expensive processes, which make the biodiesel production from sewage scum not economically feasible [56]. Furthermore, the subsequent extraction of the lipid fraction requires a significant amount of organic solvent, thus increasing the manufacturing costs [57].

Lastly, the method typically known for biodiesel production from sewage scum is based on homogeneous acid catalysts as H_2SO_4 [53–55]. Still, it is not competitive with the conventional technologies from triglycerides under alkaline catalysis for a series of drawbacks: (i) the recovery of the catalyst takes place only partially, and (ii) additional steps are required for the purification of the final products. A new methodology was then developed to successfully convert wastewater sewage scum into biodiesel, consisting of four different steps [28]. The overall process is outlined in Figure 2. First, sewage scum was heated at a temperature of 80 °C, with the lipid component was recovered by centrifugation at 4000 rpm for 3 min (recoverability > 90%), without the addition of solvents or acids [29]. Subsequently, the lipid extract was activated by adding the stoichiometric amount of formic acid (HCOOH) to calcium soaps (25–30%), thus obtaining their complete conversion into FFAs [44]. Activated lipids (FFAs = 75–80%) were then efficiently converted into the corresponding methyl esters by direct esterification using $AlCl_3 \cdot 6H_2O$ as a catalyst [45].

As a result, about 95% FFAs were converted into FAMES with minimal reactants under mild conditions (molar ratio FFAs:MeOH:catalyst = 1:10:0.02, 72 °C, 2 h). Moreover, the use of $AlCl_3 \cdot 6H_2O$ favored a convenient separation of products between the two phases: the catalyst was recovered entirely, with the upper methanol phase along with the water produced during the reaction, whereas the methyl esters were present in the lower oily phase [45]. This resultant oily phase was recovered and pure FAMES (75–80%wt) were collected by vacuum distillation (Figure 2).

The proposed scheme for exploiting sewage scum for biodiesel production has proven to be economically viable and applicable on an industrial scale. Nevertheless, the potential of the lipid component has not yet been fully exploited. After the distillation process, a residue was recovered (20–25%wt), which was analyzed by preparative chromatography. The residue was mainly composed of: ME (50.3%wt), polar compounds (33.8%), FAMES (6.4%wt) and small quantities of Me-10-HSA (3.6%wt), Mineral oils (2.7%wt), Waxes (1.8%wt), FFAs (1.0%wt) and Methyl-10-ketostearate (0.4%wt). ME already have a potential market value as biolubricants [8–10]; however, to obtain a complete valorization of the lipid component, a further improvement of the reaction by-products could help to improve the economy of the overall process. For these reasons, the transesterification reaction of ME with methanol for the synthesis of Me-10-HSA and FAMES was investigated, by optimizing the process parameters.

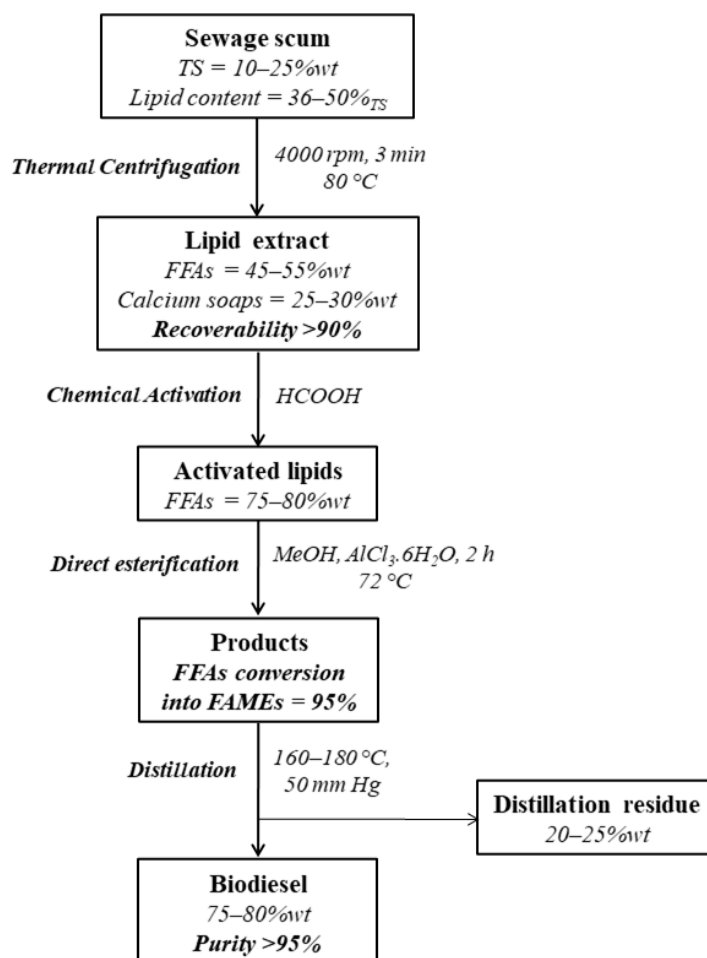


Figure 2. Scheme of biodiesel synthesis and purification from sewage scum.

2.2. Optimization of Transesterification Conditions for the Conversion of ME into Me-10-HSA and FAMES

The conversion of ME into Me-10-HSA and FAMES (according to the scheme reported in Figure 1) was optimized using $\text{AlCl}_3 \cdot 6\text{H}_2\text{O}$ and HCl as catalysts. According to the Box–Behnken experimental design described in Section 3.6 experiments were conducted on the distillation residue to find the optimal reaction conditions and study the process parameters' effect in the transesterification reaction. Experimental and predicted values for ME conversion at the design points are reported in Table 1.

A quadratic regression model was used to fit the experimental data, by obtaining the following relationships between factors and response for the two catalysts (Equations (1) and (2)):

$$\begin{aligned} \text{ME conversion } \text{AlCl}_3 \cdot 6\text{H}_2\text{O} (\%) = & -45.6167 + 11.6267C + 38.4455\text{cat} + 1.75413T + \\ & +0.410478t - 1.01146C^2 - 34.8958\text{cat}^2 - 0.00761458T^2 - 0.00848126t^2 - 2.875C\text{cat} + \\ & -0.030625CT + 0.0644231Ct + 0.203125\text{cat}T + 0.0865385\text{catt} - 0.00134615Tt \end{aligned} \quad (1)$$

$$\begin{aligned} \text{ME conversion } \text{HCl} (\%) = & 57.6733 + 10.5721C + 33.0761\text{cat} - 0.0389744T + \\ & +0.684689t - 0.404167C^2 - 10.4948\text{cat}^2 + 0.00192708T^2 - 0.000690335t^2 - 2.4375C\text{cat} + \\ & -0.054375CT + 0.00384615Ct - 0.034375\text{cat}T - 0.177885\text{catt} - 0.00442308Tt \end{aligned} \quad (2)$$

The graphs between the predicted and the experimental ME conversion (%) reported in Figure 3 show that expected values are similar to the observed values, therefore validating the model's reliability in establishing the correlation between the process variables and the ME conversion.

Table 1. Box–Behnken design matrix for the four independent variables and the experimental ME conversion (%) using $\text{AlCl}_3 \cdot 6\text{H}_2\text{O}$ and HCl as catalysts.

E	Methanol (mL)	Catalyst (mmol)	Temperature ($^{\circ}\text{C}$)	Time (h)	ME Conversion (%)			
					$\text{AlCl}_3 \cdot 6\text{H}_2\text{O}$		HCl	
					Pred.	Exp.	Pred.	Exp.
1	0	0	−1	−1	88.2	89.0	93.1	93.3
2	1	0	−1	0	94.2	94.5	86.2	84.3
3	0	1	−1	0	87.5	89.4	93.9	95.6
4	−1	0	−1	0	89.9	90.5	96.7	96.9
5	0	−1	−1	0	81.5	80.2	98.4	98.6
6	0	0	−1	1	85.3	84.3	89.3	88.6
7	0	1	0	−1	86.3	87.7	89.7	89.6
8	1	0	0	−1	95.2	94.7	95.4	95.3
9	0	−1	0	−1	94.5	92.8	95.2	96.3
10	−1	0	0	−1	87.2	87.7	96.7	96.9
11 ^a	0	0	0	0	92.9	93.4	95.3	95.5
12	−1	−1	0	0	87.7	86.6	99.9	98.1
13	1	1	0	0	97.1	97.9	94.8	93.3
14 ^a	0	0	0	0	89.9	90.5	99.6	99.7
15	1	−1	0	0	83.0	82.6	96.9	98.1
16 ^a	0	0	0	0	94.2	93.9	96.7	96.4
17	−1	1	0	0	89.3	89.2	98.7	98.5
18	0	−1	0	1	77.3	76.6	98.8	98.5
19	−1	0	0	1	80.7	82.7	98.3	98.1
20	0	1	0	1	97.2	97.5	94.8	93.3
21	1	0	0	1	86.7	85.3	97.0	96.2
22	0	0	1	−1	94.2	94.1	96.8	98.7
23	0	1	1	0	87.0	87.8	97.2	97.6
24	−1	0	1	0	94.3	95.4	99.3	99.0
25	0	−1	1	0	83.6	83.5	98.9	98.2
26	1	0	1	0	97.2	97.5	95.3	95.5
27	0	0	1	1	78.5	79.9	92.9	92.8

^a Denoted as central points. Pred. = predicted values, Exp. = experimental values.

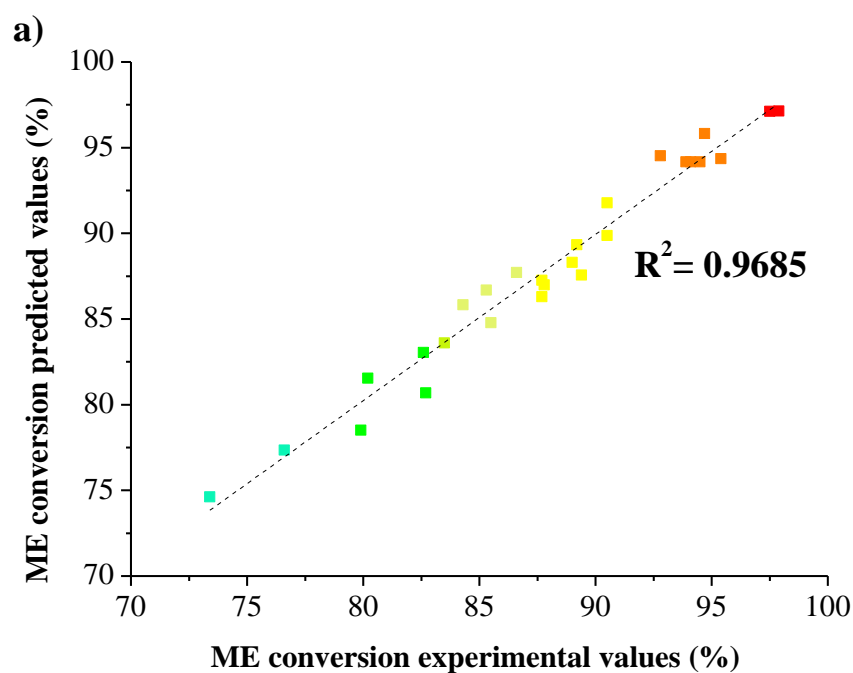


Figure 3. Cont.

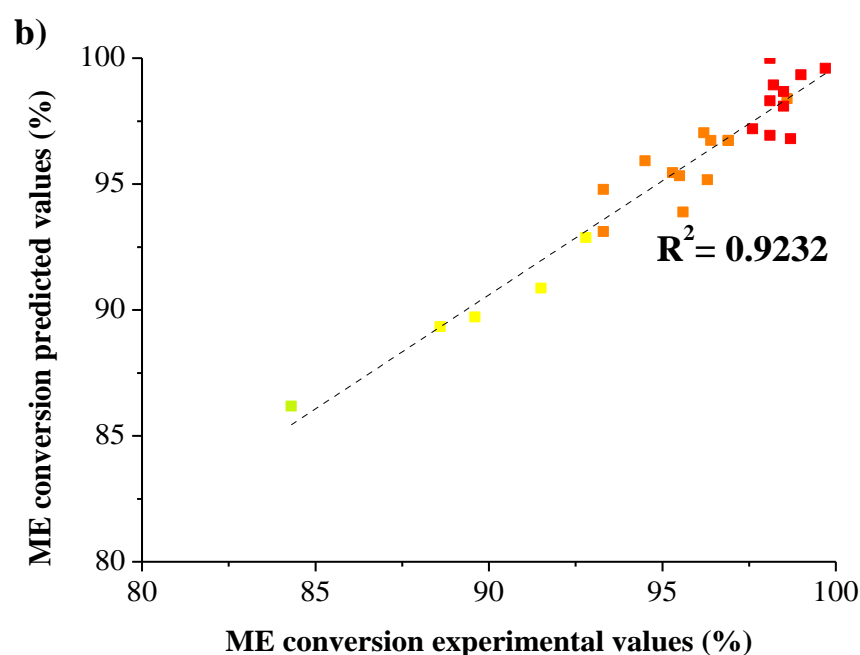


Figure 3. Predicted vs. experiment value for ME conversion (%) using (a) $\text{AlCl}_3 \cdot 6\text{H}_2\text{O}$ and (b) HCl as catalysts.

Subsequently, the significance of each parameter was evaluated by the analysis of variance (ANOVA) followed by Fisher's statistical test (F-test) for linear, interaction, and quadratic parameters in the second-order polynomial equations. In this work, the significance of the mathematical model adopted was associated with the p -value. A value of 0.05 was considered a suitable threshold with the corresponding significant parameters highlighted with an asterisk. The model's main statistics and the components of the fitting equations are given in Tables 2 and 3.

Table 2. The ANOVA summary table for the conversion of ME into Me-10-HSA and FAMEs using $\text{AlCl}_3 \cdot 6\text{H}_2\text{O}$ as catalyst.

Source	Sum of Squares	Df	Mean Square	F-Ratio	p -Value
Model	731.455	14	182.864	14.02	0.0000 *
<i>C</i>	167.253	1	167.253	64.72	0.0000 **
<i>cat</i>	181.741	1	181.741	70.33	0.0000 **
<i>T</i>	272.653	1	272.653	105.51	0.0000 **
<i>t</i>	109.808	1	109.808	42.49	0.0000 **
<i>Ccat</i>	21.16	1	21.16	8.19	0.0143 **
<i>CT</i>	6.0025	1	6.0025	2.32	0.1534
<i>Ct</i>	11.2225	1	11.2225	4.34	0.0592
<i>catT</i>	10.5625	1	10.5625	4.09	0.0661
<i>catt</i>	0.81	1	0.81	0.31	0.5859
<i>Tt</i>	0.49	1	0.49	0.19	0.6710
<i>C</i> ²	87.3001	1	87.3001	33.78	0.0001 **
<i>cat</i> ²	166.259	1	166.259	64.34	0.0000 **
<i>T</i> ²	49.4779	1	49.4779	19.15	0.0009 **
<i>t</i> ²	10.957	1	10.957	4.24	0.0619
Total error	31.0092	12	2.5841		
Total (corr.)	1018.31	26			

$R^2 = 96.95\%$ * $p < 0.05$ indicates model is significant. $R^2(\text{adjusted for d.f.}) = 93.39\%$ ** $p < 0.05$ indicates model terms are significant

Table 3. The ANOVA summary table for the conversion of ME into Me-10-HSA and FAMEs using HCl as catalyst.

Source	Sum of Squares	Df	Mean Square	F-Ratio	<i>p</i> -Value
Model	236.882	14	59.2204	11.79	0.0000 *
<i>C</i>	82.6875	1	82.6875	35.10	0.0001 **
<i>cat</i>	86.4033	1	86.4033	36.67	0.0001 **
<i>T</i>	36.75	1	36.75	15.60	0.0019 **
<i>t</i>	31.0408	1	31.0408	13.17	0.0035 **
<i>Ccat</i>	15.21	1	15.21	6.46	0.0259 **
<i>CT</i>	18.9225	1	18.9225	8.03	0.0151 **
<i>Ct</i>	0.04	1	0.04	0.02	0.8985
<i>catT</i>	0.3025	1	0.3025	0.13	0.7263
<i>catt</i>	3.4225	1	3.4225	1.45	0.2513
<i>Tt</i>	5.29	1	5.29	2.25	0.1599
<i>C</i> ²	13.9393	1	13.9393	5.92	0.0316 **
<i>cat</i> ²	15.0379	1	15.0379	6.38	0.0266 **
<i>T</i> ²	3.16898	1	3.16898	1.35	0.2687
<i>t</i> ²	0.0725926	1	0.0725926	0.03	0.8636
Total error	28.2725	12	2.35604		
Total (corr.)	347.365	26			

$R^2 = 93.32\%$ * $p < 0.05$ indicates model is significant. $R^2(\text{adjusted for d.f.}) = 90.46\%$ ** $p < 0.05$ indicates model terms are significant.

The *p*-associated values for the models adopted were less than 0.05, indicating that the model used to describe the transesterification reaction of ME with methanol was statistically significant. All linear parameters were substantial in the transesterification process. In particular, it was noted that there was a considerable difference in the relationship between the independent variables and their effects on the response variable (ME conversion) for the two catalysts. Using $\text{AlCl}_3 \cdot 6\text{H}_2\text{O}$ as a catalyst, temperature showed the most significant impact in the transesterification reaction followed by the amount of the catalyst, methanol and reaction time (Table 2). Instead, in the case of HCl, the amount of catalyst and methanol were the most significant variables with respect to temperature and reaction time (Table 3). As for the other terms (interaction and quadratic parameters), only *Ccat* (the interaction between the amount of methanol and catalyst), *C*² (the quadratic term associated with the methanol amount) and *cat*² (the quadratic term related to the amount of catalyst) were significant for both catalysts. Then, the goodness of fit of the models was checked by the coefficient of determination R^2 . The value obtained of 0.9339 and 0.9046, respectively, for $\text{AlCl}_3 \cdot 6\text{H}_2\text{O}$ and HCl in its adjusted form, confirmed the efficacy of the model adopted.

Finally, response surface plots were generated to investigate the influence of the process parameters in the conversion of ME and identify the optimal experimental conditions required for both catalysts. Figure 4a shows the combined effect of methanol and catalyst, at a fixed temperature of 100 °C and a reaction time of 17 h. By increasing the amount of methanol and catalyst, an increase of conversion of ME was observed: 95 and 100%, were respectively obtained for $\text{AlCl}_3 \cdot 6\text{H}_2\text{O}$ and HCl with 5 mL of methanol and 1 mmol of catalyst. In Figure 4b, the effect of the temperature with the reaction time was investigated (methanol = 3 mL, catalyst = 0.6 mmol). In this case, the key role played by temperature in the transesterification reaction for the two systems studied is clear. At 120 °C, for $\text{AlCl}_3 \cdot 6\text{H}_2\text{O}$, the transesterification process's kinetic was particularly slow and long reaction times (30 h) were required for the full conversion of ME. In contrast, the reaction was complete after a few hours (4–6 h) using HCl. Figure 4c,d show the combined effect of temperature and catalyst (methanol = 3 mL, time = 17 h) and reaction time and methanol (catalyst = 0.6 mmol, temperature = 100 °C), respectively. These combinations of factors positively influenced the conversion of ME, obtaining a value close to 100%.

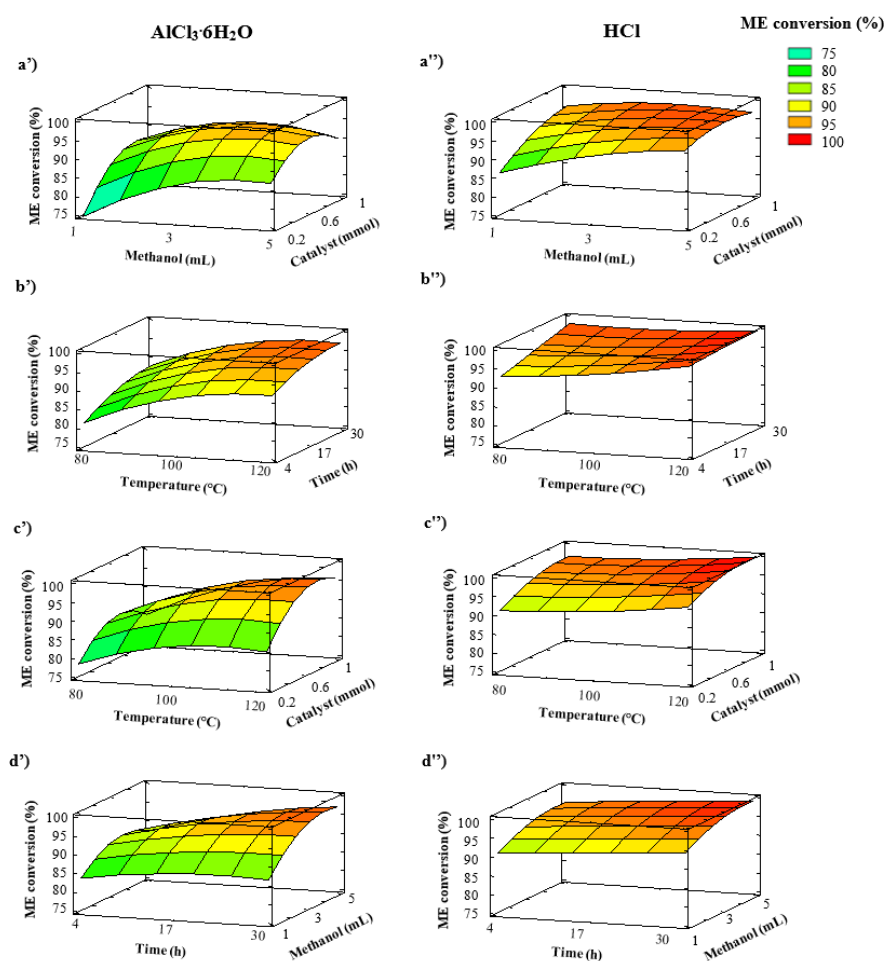


Figure 4. Response surface plot of the combined effects of: (a) methanol and catalyst amount (temperature = 100 °C, time = 17 h), (b) temperature and reaction time (methanol = 3 mL, catalyst = 0.6 mmol), (c) temperature and catalyst (methanol = 3 mL, time = 17 h), (d) time and methanol (catalyst = 0.6 mmol, temperature = 100 °C) for $\text{AlCl}_3 \cdot 6\text{H}_2\text{O}$ and HCl.

Based on these results, the optimal conditions were determined and directly applied in the transesterification of ME with methanol. The results obtained are reported in Table 4. Predicted responses are found to be in good agreement with the experimental results. In detail, using $\text{AlCl}_3 \cdot 6\text{H}_2\text{O}$ as a catalyst (0.76 mmol), a ME conversion of 99.6% was obtained at 115 °C after 30 h of reaction and 3.9 mL of methanol. Instead, the reaction catalyzed by HCl (1 mmol) was much faster: a ME conversion of 99.8% was achieved at 120 °C with a reduced amount of methanol (2.1 mL) after 4 h. In the absence of the catalyst, using the highest amount of methanol (5 mL) at 120 °C, a ME conversion of only 3% was obtained, confirming the efficiency of both catalysts.

Table 4. Results of the model validation under optimum conditions using $\text{AlCl}_3 \cdot 6\text{H}_2\text{O}$ and HCl as catalysts.

Catalysts	Methanol (mL)	Amount (mmol)	Temperature (°C)	Time (h)	ME Conversion (%)	
					Pred.	Exp.
$\text{AlCl}_3 \cdot 6\text{H}_2\text{O}$	3.9	0.76	115	30	99.4	99.6
HCl	2.1	1	120	4	100	99.8

Pred. = predicted values, Exp. = experimental values.

The transesterification in methanol of stearyl stearate was also evaluated to compare the different reactivity between HCl and $\text{AlCl}_3 \cdot 6\text{H}_2\text{O}$ vs. a fatty ester less congested sterically.

As can be seen from Table 5, for both the catalysts, a total conversion of stearyl stearate in methyl stearate was obtained at 100 °C after 24 h. In the case of HCl catalysis, the conversion is high even after 2 h at 70 °C (80%), showing a higher reaction rate than that of $\text{AlCl}_3 \cdot 6\text{H}_2\text{O}$, for which the conversion was only about 20%. Furthermore, regarding $\text{AlCl}_3 \cdot 6\text{H}_2\text{O}$, the results obtained clearly show that the amounts of methanol and catalyst greatly influence the transformation of stearyl stearate. This different behavior could be ascribed to the different strength of acidity among these two catalysts and the higher steric hindrance related to the hexa-aquo complex of aluminum chloride [45]. In fact, it was already demonstrated that the partial substitution of water coordinated to the aluminum center in $\text{AlCl}_3 \cdot 6\text{H}_2\text{O}$ produces a mixed-aquo-alcohol complex, which acts as a Brønsted acid.

Table 5. Stearyl stearate conversions under HCl and $\text{AlCl}_3 \cdot 6\text{H}_2\text{O}$ catalysis.

	HCl		$\text{AlCl}_3 \cdot 6\text{H}_2\text{O}$	
	70 °C, 2 h	100 °C, 24 h	70 °C, 2 h	100 °C, 24 h
Conversion (%)	80	100	20	100

2.3. Analysis of the Reaction Products

Once identified the optimal experimental conditions required for the complete conversion of ME, the organic phase was processed by column chromatography [28] and the products obtained were isolated, analyzed and quantified (Figures S1–S8). Based on 100 g of distillation residue, 28.2 g FAMEs and 32.3 g Me-10-HSA were respectively achieved. A detailed analysis of the fatty acids (FAs) profile was carried out by comparing the chemical composition of the methyl esters obtained with that of biodiesel previously recovered from FAME distillation. The results are reported in Figure 5.

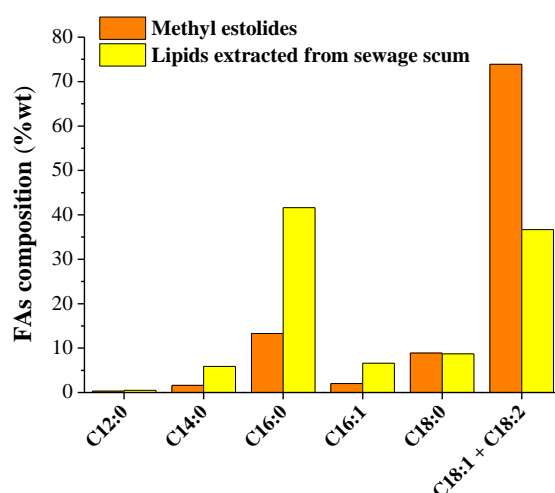


Figure 5. Comparison of FAs profile (%wt.) of methyl estolides and lipids extracted from sewage scum.

ME contained predominately oleic acid (C18:1) and linoleic acid (C18:2), totaling 73.9% of fatty acids present (AMW FAs = 276.8 g/mole). Instead, the distilled biodiesel from sewage scum (Figure 2) showed nearly equal amounts of saturated fatty acid and unsaturated fatty acid (AMW FAs = 266.8 g/mole) (Figure S9). This difference in FAs profile can be attributed to a possible origin of estolides as reaction products between 10-HSA (obtained from the enantioselective microbial hydration of oleic acid [25]) the subsequent esterification and/or transesterification with the oils and fats present in the stream. Considering only the market value of biodiesel produced (EUR 0.8 kg⁻¹ [58]), a

potential gain of EUR 225 could be obtained for each ton of the sample treated, leading to a further enhancement of sewage sludge to produce biofuels and biochemicals. However, the greatest profits would be obtained from Me-10-HSA produced during the process.

A high enantiomeric excess ($ee > 92\%$) of R-enantiomeric form was observed (Figure S10), compound employed as the precursor to produce biochemicals, namely γ -(R)-dodecalactone. Since its current market value ranges from EUR 800 to 3000 kg^{-1} [59], the economy of the whole process would be greatly improved. As described above, the synthesis of 10-HSA generally requires the use of enzymes. The use of HCl or $\text{AlCl}_3 \cdot 6\text{H}_2\text{O}$ as a catalyst not only is significantly cheaper (EUR 0.8 kg^{-1} [60]), but in the case of $\text{AlCl}_3 \cdot 6\text{H}_2\text{O}$ at the end of its use, it could potentially be used in WWTPs as a coagulant, further contributing to the overall economy of the process.

3. Materials and Methods

3.1. Reagents and Instruments

All chemical reagents used in this work were of analytical grade and were used directly without further purification or treatment. Hexane (C_6H_{14} , 99%), toluene (C_6H_6 , 99%), methanol (CH_3OH , 99.8%) and methyl heptadecanoate ($\text{C}_{18}\text{H}_{36}\text{O}_2$, $\geq 99\%$) were purchased from Sigma-Aldrich. Aluminum chloride hexahydrate ($\text{AlCl}_3 \cdot 6\text{H}_2\text{O}$, 99%) was obtained as pure-grade reagent from Baker. Ethanol ($\text{C}_2\text{H}_5\text{OH}$, $\geq 99.8\%$), diethyl ether ($(\text{C}_2\text{H}_5)_2\text{O}$, 99%), formic acid (HCOOH , 99%), sulfuric acid (H_2SO_4 , 98%), hydrochloric acid (HCl, 37%) and potassium hydroxide (KOH, 85%) were purchased from Carlo Erba.

A Rotofix 32 Hettich Centrifuge was used for the centrifugation experiments.

Identification of ME, Me-10-HSA and FAMEs was carried out by gas chromatography-mass spectroscopy (GC-MS) using a Perking Elmer Clarus 500 equipped with a Clarus spectrometer. Quantitative determinations were performed using a Varian 3800 GC-FID. Helium was used as a carrier gas with a flow of 1.3 mL min^{-1} . Both instruments were configured for cold on-column injections with a HP-5MS capillary column (30 m; Ø 0.32 mm; 0.25 μm film). The same temperature program was employed for the injector and the oven. The initial temperature was set to 60 $^\circ\text{C}$ and kept constant for 2 min. Then, it increased to 300 $^\circ\text{C}$ with a 15 $^\circ\text{C min}^{-1}$ ramp and kept constant for other 20 min. The temperature of detector (FID) was set to 300 $^\circ\text{C}$. For GC-MS, the ion source was set to 70 eV and maintained at 250 $^\circ\text{C}$.

FTIR spectra were recorded by a Perkin Elmer FTIR Spectrum BX instrument using KBr cells (neat compounds).

^1H NMR spectra were recorded on a Bruker AV-400 spectrometer using the residual solvent peak as a reference [61].

3.2. Sewage Scum

Sewage scum was collected from WWTPs of Bari West (240,000 Population Equivalent, PE), located in South of Italy. Samples were immediately processed to avoid long storage time (within two days, 4 $^\circ\text{C}$) and characterized in terms of total solids, lipids, proteins, cellulose, lignin and ashes [29].

3.3. Experimental Procedure for Lipids Characterization

3.3.1. Determination of FFAs and Soaps

FFAs were determined by titration of the acidity present with a 0.1 N KOH solution and phenolphthalein ($\geq 99\%$, Sigma-Aldrich) as an indicator. A total of 1 g of the sample collected was previously dissolved into 150 mL of a 1:1 *v/v* diethyl ether:ethanol mixture. Using the same experimental conditions, soaps were determined by titration with a 0.1 N HCl solution and methyl red (99%, Sigma-Aldrich) as an indicator.

3.3.2. Determination of Fatty Acids Profile and Average Molecular Weight

In a glass Pyrex reactor of 5 mL, 0.02 g of sample were dissolved with 2 mL of a 2:2:0.01 *v/v/v* toluene:methanol:concentrated H_2SO_4 solution. The system was closed

and placed into an ultrasonic bath at 70 °C for 5 h. Then, 1 mL of methyl heptadecanoate toluene solution (1000 ppm) was added as internal standard and the resulting solution gas-chromatographically analyzed (1 µL). Average molecular weight (AMW) was determined according to the following equation (Equation (3)):

$$AMW = \frac{\sum A_i MW_i}{\sum A_i} \quad (3)$$

where A_i and MW_i are the area and molecular weight of FFAs identified, respectively. Then, FAMEs content (%wt.) was calculated respect to methyl heptadecanoate as follows (Equation (4)):

$$FAMEs \text{ content} = \frac{\sum A_i}{A_{sdt}} \times \frac{m_{sdt}}{m_{sample}} \times 100 \quad (4)$$

where A_{sdt} and m_{sdt} are the area and the mass of standard (methyl heptadecanoate), respectively, and m_{sample} is the amount of sample analyzed.

3.4. Extraction of Lipid Fraction from Sewage Scum and Chemical Activation

In a glass Pyrex reactor of 250 mL, 100 g of sewage scum were placed and closed. The system was heated in an oven at 80 °C. After this thermal treatment, the sample was rapidly centrifuged at 4000 rpm for 3 min by obtaining a three-phasic system consisting of: (i) an upper organic brown oily phase, (ii) a lower phase of wet residual solid, and (iii) an aqueous intermediate phase. The oily phase was recovered and stored at 4 °C for the subsequent operations. The isolated product was mainly constituted by FFAs (51.7%wt) and calcium soaps of fatty acids (30.4%wt). Then, the stoichiometric amount of HCOOH respect to the calcium soaps was added (4.8 g for 100 g of raw lipids) and the activated lipids recovered as clear oil, after centrifugation (4000 rpm, 1 min) at 80 °C [44].

3.5. Conversion of Activated Lipids into Methyl Esters of Recovery of Biodiesel Produced by Distillation Process

Activated lipids extracted from sewage scum were converted into the corresponding methyl esters, by direct esterification with methanol using $AlCl_3 \cdot 6H_2O$ as a catalyst [45]. The reaction was carried out at 72 °C for 2 h with a molar ratio FFAs:MeOH:catalyst = 1:10:0.02. At the end of the process, the reagent mixture was cooled to room temperature with the formation of bi-phasic system consisting of: (i) a light methanol layer (in which the catalyst was present) and (ii) a lower oily layer composed of methyl esters. The oily phase was recovered, and the residual methanol removed under vacuum (60 °C, 700 mmHg). Finally, biodiesel (75–80%wt, purity > 99%) was collected by subsequently vacuum distillation (160–180 °C, 50 mm Hg). The distillation residue (20–25%wt) was instead recovered, dried under nitrogen flow and analyzed by column chromatography [29], obtaining the chemical composition reported in Table 6.

Table 6. Chemical composition of the distillation residue obtained after direct esterification of the lipid fraction with methanol and recovery of biodiesel produced by distillation process.

Chemical Species	Composition (%wt.)
Mineral oil	2.7
Waxes	1.8
FAMEs	6.4
Me-10-HAS	3.6
Methyl-10-ketostearate	0.4
Methyl estolides	50.3
Acids	1.0
Other polar compounds	33.8

3.6. Transesterification Reaction of Methyl Estolides (or Stearyl Stearate) with Methanol

In a typical reaction, 0.1 g of sample (the distillation residue recovered in the previous step, ME content = 50.3% or stearyl stearate) were placed with methanol (1 mL) and 0.2 mmol of catalyst (HCl or $\text{AlCl}_3 \cdot 6\text{H}_2\text{O}$) in a glass Pyrex reactor of 15 mL. The system was closed and placed into a thermostatic bath at 80 °C for 4 h under agitation (250 rpm), using a magnetic stirring. Then, it was cooled to room temperature and the residual methanol was removed under nitrogen flow. Where it was possible, the catalyst was recovered by centrifugation and the organic phase was analyzed by gas chromatography for the determination of FAMES content. Following the same procedure, Me-10-HSA and ME were also determined with the calibration curves obtained from the pure product, previously isolated by column chromatography [28].

Optimization of Transesterification Conditions

A three-step approach was used to investigate the effects of the process variables in the conversion of ME into Me-10-HSA and FAMES and maximize their yield [44]. Methanol (C) and catalyst (cat) amount, temperature (T) and reaction time (t) were selected as independent variables (factors), while methyl estolides (ME) conversion was set as dependent variable (response). The experimental range of the levels and the independent variables considered in this study are presented in Table 7.

Table 7. Experimental range and levels of independent variables.

Variables	Symbol	Range and Levels			ΔX_i ^a
		Lower Level (−1)	Center Level (0)	Upper Level (+1)	
Methanol (mL)	C	1	3	5	2
Catalyst (mmol)	cat	0.2	0.6	1	0.4
Temperature (°C)	T	80	100	120	20
Time (h)	t	4	17	30	13

^a Step change values.

A total of 27 experiments (including three replicates for the center point), were used for fitting a second-order response surface. The effects of factors on the response were analyzed according to the following quadratic function (Equation (5)):

$$Y = \beta_0 + \sum_{i=1}^n \beta_i X_i + \sum_{i=1}^n \beta_{ii} X_i^2 + \sum_{i=1}^n \sum_{i < j}^n \beta_{ij} X_i X_j \quad (5)$$

where Y represents the ME conversion (%), X_i and X_j are the independent variables, β_0 , β_i , β_{ij} and β_{ii} are the offset term, linear, interaction, and quadratic parameters, respectively. Statgraphycs® Centurion XVI was used for the regression analysis and the plot response surface. Then, to verify the validation of the overall fit of the developed regression model, the data obtained were processed by the analysis of variance (ANOVA). The adequacy of the polynomial model to fit experimental data were expressed as R^2 (coefficient of determination) and in its adjusted form. The statistical significance of R^2 was checked by the F-test at a confidence level of 95%.

Finally, the optimization of reaction conditions was carried out using response surface methodology (RSM) combined with the desirability function approach to form the desirability optimization methodology (DOM) [45].

4. Conclusions

In this work, for the first time, an efficient method was proposed for the synthesis of Me-10-HSA and FAMES by direct conversion of methyl estolides isolated from sewage scum. A response surface methodology was applied to investigate the effect of the process variables on the methyl estolides conversion and maximize the final yield. $\text{AlCl}_3 \cdot 6\text{H}_2\text{O}$

and HCl were used as effective catalysts in promoting transesterification with methanol. HCl is more active in promoting the transesterification of methyl estolides to produce FAMEs and Me-(*R*)-10-HSA: a total conversion was in fact obtained already after 4 h. In the case of $\text{AlCl}_3 \cdot 6\text{H}_2\text{O}$, under similar reactive conditions, 20 h were necessary to achieve a conversion of 99.4%. On the other side, $\text{AlCl}_3 \cdot 6\text{H}_2\text{O}$ is a solid catalyst, easy to manage and less corrosive than mineral conventional acids [62]. $\text{AlCl}_3 \cdot 6\text{H}_2\text{O}$ -catalyzed reaction resulted principally affected by temperature, whereas in the case of HCl, the amount of catalyst and methanol were the most significant variables. The obtainment of Me-(*R*)-10-HSA, in its (almost) pure enantiomeric form, increases the potential of sewage scum. For the specific case of $\text{AlCl}_3 \cdot 6\text{H}_2\text{O}$, the possible final use of the relevant residues in WWTPs as a coagulant results in a new scheme of valorization of a special waste, namely sewage scum, in which no secondary waste was generated. The transesterification of methyl estolides could actually implement the scenario of the full valorization of sewage scum towards a multi-products biorefinery. With the use of a limited number of reagents namely MeOH and $\text{AlCl}_3 \cdot 6\text{H}_2\text{O}$, and an integrated network of processes, biodiesel, methyl estolides, and Me-(*R*)-10-HSA would be effectively obtained from sewage scum in a sustainable way.

Supplementary Materials: The following are available online at <https://www.mdpi.com/article/10.3390/catal11060663/s1>, Figure S1: GC-chromatogram of methyl estolides isolated by distillation process, Figure S2: FTIR spectra of methyl estolides, Figure S3: GC-MS chromatogram of 10-(palmitoyloxy)-stearic methyl ester, Figure S4: GC-MS chromatogram of 10-(stearoyloxy)-stearic methyl ester, Figure S5: GC-chromatogram of methyl 10-(*R*)-hydroxystearate isolated, Figure S6: FTIR spectra of methyl 10-(*R*)-hydroxystearate, Figure S7: GC-MS chromatogram of methyl 10-(*R*)-hydroxystearate, Figure S8: ^1H NMR of isolated methyl 10-(*R*)-hydroxystearate, Figure S9: Comparison of chromatographic profiles of FAs obtained from methyl estolides and lipids extracted from sewage scum, Figure S10: Chemical structures of derivatizing agents (D1, D2 and D3) used for the determination of the absolute configuration of the Methyl 10-Hydroxy stearic acid (M10-HSA) isolated from sewage scum.

Author Contributions: L.d.B.: Methodology, Writing—original draft, Investigation, Validation. V.D.: Methodology, Writing—original draft, Investigation. C.P.: Conceptualization, Methodology, Investigation, Resources, Writing—review & editing, Supervision, Project administration, Funding acquisition. All authors have read and agreed to the published version of the manuscript.

Funding: This study was financially supported by MIUR (ERANETMEDNEXUS-14-035 Project WE-MET). This research was partially supported by European Union—FESR “PON Ricerca e Innovazione 2014–2020. Progetto: Energie per l’Ambiente TARANTO—Cod. ARS01_00637”.

Data Availability Statement: The data presented in this study are contained within the article and the supplementary material.

Conflicts of Interest: The authors declare no conflict of interest.

Abbreviations

Roman Letters

A_i	Gas-chromatographic area of fatty acids detected
$\text{AlCl}_3 \cdot 6\text{H}_2\text{O}$	Aluminum Chloride Hexahydrate
A_{std}	Area of standard (methyl heptadecanoate)
C	Amount of Methanol
Cat	Amount of catalyst ($\text{AlCl}_3 \cdot 6\text{H}_2\text{O}$ or HCl)
$\text{C}_2\text{H}_5\text{OH}$	Ethanol
$\text{C}_{18}\text{H}_{36}\text{O}_2$	Methyl heptadecanoate
CH_3OH	Methanol
$(\text{C}_2\text{H}_5)_2\text{O}$	Diethyl ether
C_6H_{14}	Hexane
C_7H_8	Toluene

FAMEs	Fatty Acid Methyl Esters
FAs	Fatty Acids
FFAs	Free Fatty Acids
HCOOH	Formic acid
HCl	Hydrochloric Acid
HFAs	Hydroxy Fatty Acids
10-HAS	10-(R)-Hydroxystearic acid
H ₂ SO ₄	Sulfuric acid
KOH	Potassium hydroxide
m _{sample}	Mass of sample analyzed
m _{std}	Mass of standard (methyl heptadecanoate)
ME	Methyl Estolides
Me-10-HAS	Methyl 10-(R)-Hydroxystearate
MW _i	Molecular weight of fatty acids detected
T	Temperature
TS	Total Solids
T	Time
X _i , X _j	Independent variables
Y	Dependent variable
Greek Letters	
β ₀	Offset term
β _i , β _{ij} , β _{ii}	Linear, interaction, and quadratic parameters

References

- Löwe, J.; Gröger, H. Fatty Acid Hydratases: Versatile Catalysts to Access Hydroxy Fatty Acids in Efficient Syntheses of Industrial Interest. *Catalysts* **2020**, *8*, 287. [\[CrossRef\]](#)
- Cao, Y.; Zhang, X. Production of long-chain hydroxy fatty acids by microbial conversion. *Appl. Microbiol. Biotechnol.* **2013**, *97*, 3323–3331. [\[CrossRef\]](#) [\[PubMed\]](#)
- Kolar, M.J.; Konduri, S.; Chang, T.; Wang, H.; McNerlin, C.; Ohlsson, L.; Härröd, M.; Siegel, D.; Saghatelian, A. Linoleic acid esters of hydroxy linoleic acids are anti-inflammatory lipids found in plants and mammals. *J. Biol. Chem.* **2019**, *294*, 10698–10707. [\[CrossRef\]](#) [\[PubMed\]](#)
- Rodríguez, J.P.; Guijas, C.; Astudillo, A.M.; Rubio, J.M.; Balboa, M.A.; Balsinde, J. Sequestration of 9-Hydroxystearic Acid in FAHFA (Fatty Acid Esters of Hydroxy Fatty Acids) as a Protective Mechanism for Colon Carcinoma Cells to Avoid Apoptotic Cell Death. *Cancers* **2019**, *11*, 524. [\[CrossRef\]](#) [\[PubMed\]](#)
- Suriyamongkol, P.; Weselake, R.; Narine, S.; Moloney, M.; Shah, S. Biotechnological approaches for the production of polyhydroxyalkanoates in microorganisms and plants—A review. *Biotechnol. Adv.* **2007**, *25*, 148–175. [\[CrossRef\]](#)
- Verlinden, R.A.; Hill, D.J.; Kenward, M.A.; Williams, C.D.; Radecka, I. Bacterial synthesis of biodegradable polyhydroxyalkanoates. *J. Appl. Microbiol.* **2007**, *102*, 1437–1449. [\[CrossRef\]](#)
- Chen, Y.; Biresaw, G.; Cermak, S.C.; Isbell, T.A.; Ngo, H.L.; Chen, L.; Durham, A.L. Fatty Acid Estolides: A Review. *J. Am. Oil Chem. Soc.* **2020**, *97*, 231–241. [\[CrossRef\]](#)
- Cecilia, J.A.; Plata, D.B.; Maria, R.; Saboya, A.; Murilo, F.; De Luna, T.; Cavalcante, C.L.; Rodríguez-castellón, E. An Overview of the Biolubricant Production Process: Challenges and Future Perspectives. *Processes* **2020**, *8*, 257. [\[CrossRef\]](#)
- De Haro, J.C.; Garrido, M.D.P.; Ángel, P.; Carmona, M.; Rodríguez, J.F. Full conversion of oleic acid to estolides esters, biodiesel and choline carboxylates in three easy steps. *J. Clean. Prod.* **2018**, *184*, 579–585. [\[CrossRef\]](#)
- McNutt, J.; He, Q. (Sophia) Development of biolubricants from vegetable oils via chemical modification. *J. Ind. Eng. Chem.* **2016**, *36*, 1–12. [\[CrossRef\]](#)
- Boratyński, F.; Szczepańska, E.; De Simeis, D.; Serra, S.; Brenna, E. Bacterial Biotransformation of Oleic Acid: New Findings on the Formation of γ -Dodecalactone and 10-Ketostearic Acid in the Culture of *Micrococcus Luteus*. *Molecules* **2020**, *25*, 3024. [\[CrossRef\]](#) [\[PubMed\]](#)
- Kourist, R.; Hilterhaus, R. Microbial lactone synthesis based on renewable resources. In *Microorganisms in Biorefineries*; Springer: Berlin/Heidelberg, Germany, 2015; pp. 275–301.
- An, J.-U.; Joo, Y.-C.; Oh, D.-K. New Biotransformation Process for Production of the Fragrant Compound γ -Dodecalactone from 10-Hydroxystearate by Permeabilized *Waltomyces lipofer* Cells. *Appl. Environ. Microbiol.* **2013**, *79*, 2636–2641. [\[CrossRef\]](#) [\[PubMed\]](#)
- Soni, S.; Agarwal, M. Lubricants from renewable energy sources—A review. *Green Chem. Lett. Rev.* **2014**, *7*, 359–382. [\[CrossRef\]](#)
- Yao, L.; Hammond, E.G.; Wang, T.; Bhuyan, S.; Sundararajan, S. Synthesis and physical properties of potential biolubricants based on ricinoleic acid. *J. Am. Oil Chem. Soc.* **2010**, *87*, 937–945. [\[CrossRef\]](#)
- Hiseni, A.; Arends, I.W.C.E.; Otten, L.G. New Cofactor-Independent Hydration Biocatalysts: Structural, Biochemical, and Biocatalytic Characteristics of Carotenoid and Oleate Hydratases. *ChemCatChem* **2014**, *7*, 29–37. [\[CrossRef\]](#)

17. Jenkins, T.C.; AbuGhazaleh, A.A.; Freeman, S.; Thies, E.J. The Production of 10-Hydroxystearic and 10-Ketostearic Acids Is an Alternative Route of Oleic Acid Transformation by the Ruminant Microbiota in Cattle. *J. Nutr.* **2006**, *136*, 926–931. [[CrossRef](#)]
18. Chen, Y.Y.; Liang, N.Y.; Curtis, J.M.; Gänzle, M.G. Characterization of Linoleate 10-Hydratase of *Lactobacillus plantarum* and Novel Antifungal Metabolites. *Front. Microbiol.* **2016**, *7*, 1561. [[CrossRef](#)]
19. Kim, B.-N.; Joo, Y.-C.; Kim, Y.-S.; Kim, K.-R.; Oh, D.-K. Erratum to: Production of 10-hydroxystearic acid from oleic acid and olive oil hydrolyzate by an oleate hydratase from *Lysinibacillus fusiformis*. *Appl. Microbiol. Biotechnol.* **2012**, *95*, 1095–1096. [[CrossRef](#)]
20. Kim, K.-R.; Kang, W.-R.; Oh, D.-K. Complete genome sequence of *Stenotrophomonas* sp. KACC 91585, an efficient bacterium for unsaturated fatty acid hydration. *J. Biotechnol.* **2017**, *241*, 108–111. [[CrossRef](#)] [[PubMed](#)]
21. Hudson, J.A.; MacKenzie, C.A.M.; Joblin, K.N. Conversion of oleic acid to 10-hydroxystearic acid by two species of ruminal bacteria. *Appl. Microbiol. Biotechnol.* **1995**, *44*, 1–6. [[CrossRef](#)]
22. Kang, W.-R.; Seo, M.-J.; Shin, K.-C.; Park, J.-B.; Oh, D.-K. Gene cloning of an efficiency oleate hydratase from *Stenotrophomonas nitritireducens* for polyunsaturated fatty acids and its application in the conversion of plant oils to 10-hydroxy fatty acids. *Biotechnol. Bioeng.* **2017**, *114*, 74–82. [[CrossRef](#)] [[PubMed](#)]
23. Kang, W.R.; Seo, M.J.; Shin, K.C.; Park, J.B.; Oh, D.K. Comparison of biochemical properties of the original and newly identified oleate hydratases from *Stenotrophomonas maltophilia*. *Appl. Environ. Microbiol.* **2017**, *83*. [[CrossRef](#)]
24. Kuo, T.M.; Lanser, A.C.; Nakamura, L.K.; Hou, C.T. Production of 10-ketostearic acid and 10-hydroxystearic acid by strains of *Sphingobacterium thalophilum* isolated from composted manure. *Curr. Microbiol.* **2000**, *40*, 105–109. [[CrossRef](#)]
25. Serra, S.; De Simeis, D.; Castagna, A.; Valentino, M. The Fatty-Acid Hydratase Activity of the Most Common Probiotic Microorganisms. *Catalysts* **2020**, *10*, 154. [[CrossRef](#)]
26. Hou, C.T. Biotechnology for fats and oils: New oxygenated fatty acids. *New Biotechnol.* **2009**, *26*, 2–10. [[CrossRef](#)] [[PubMed](#)]
27. Pera, L.M.; Baigori, M.D.; Pandey, A.; Castro, G.R. Biocatalysis. In *Industrial Biorefineries & White Biotechnology*; Elsevier: Amsterdam, The Netherlands, 2015; pp. 391–408. [[CrossRef](#)]
28. Di Bitonto, L.; Todisco, S.; Gallo, V.; Pastore, C. Urban sewage scum and primary sludge as profitable sources of biodiesel and biolubricants of new generation. *Bioresour. Technol. Rep.* **2020**, *9*, 100382. [[CrossRef](#)]
29. Di Bitonto, L.; Lopez, A.; Mascolo, G.; Mininni, G.; Pastore, C. Efficient solvent-less separation of lipids from municipal wet sewage scum and their sustainable conversion into biodiesel. *Renew. Energy* **2016**, *90*, 55–61. [[CrossRef](#)]
30. Di Bitonto, L.; Locaputo, V.; D’Ambrosio, V.; Pastore, C. Direct Lewis-Brønsted acid ethanolysis of sewage sludge for production of liquid fuels. *Appl. Energy* **2020**, *259*, 114163. [[CrossRef](#)]
31. Casiello, M.; Catucci, L.; Fracassi, F.; Fusco, C.; Laurenza, A.G.; Di Bitonto, L.; Pastore, C.; D’Accolti, L.; Nacci, A. ZnO/Ionic Liquid Catalyzed Biodiesel Production from Renewable and Waste Lipids as Feedstocks. *Catalysts* **2019**, *9*, 71. [[CrossRef](#)]
32. *Urban Waste Grease Resource Assessment*; NREL: Golden, CO, USA, 1998; NREL/SR-570-26141.
33. Igoni, A.H.; Ayotamuno, M.; Eze, C.; Ogaji, S.; Probert, S. Designs of anaerobic digesters for producing biogas from municipal solid-waste. *Appl. Energy* **2008**, *85*, 430–438. [[CrossRef](#)]
34. Bertanza, G.; Canato, M.; Laera, G.; Tomei, M.C. Methodology for technical and economic assessment of advanced routes for sludge processing and disposal. *Environ. Sci. Pollut. Res.* **2014**, *22*, 7190–7202. [[CrossRef](#)] [[PubMed](#)]
35. Chipasa, K.B.; Mdrzycka, K. Characterization of the fate of lipids in activated sludge. *J. Environ. Sci.* **2008**, *20*, 536–542. [[CrossRef](#)]
36. Di Bitonto, L.; Pastore, C. Up-grading of Waste Oil: A Key Step in the Future of Biofuel Production. In *Process Systems Engineering for Biofuels Development*; John Wiley & Sons: New York, NY, USA, 2020; pp. 121–147. [[CrossRef](#)]
37. Huang, Y.; Li, Y.; Han, X.; Zhang, J.; Luo, K.; Yang, S.; Wang, J. Investigation on fuel properties and engine performance of the extraction phase liquid of bio-oil/biodiesel blends. *Renew. Energy* **2020**, *147*, 1990–2002. [[CrossRef](#)]
38. Lawan, I.; Zhou, W.; Idris, A.L.; Jiang, Y.; Zhang, M.; Wang, L.; Yuan, Z. Synthesis, properties and effects of a multi-functional biodiesel fuel additive. *Fuel Process. Technol.* **2020**, *198*, 106228. [[CrossRef](#)]
39. Tamilselvan, P.; Nallusamy, N.; Rajkumar, S. A comprehensive review on performance, combustion and emission characteristics of biodiesel fuelled diesel engines. *Renew. Sustain. Energy Rev.* **2017**, *79*, 1134–1159. [[CrossRef](#)]
40. Singh, D.; Sharma, D.; Soni, S.; Sharma, S.; Sharma, P.K.; Jhalani, A. A review on feedstocks, production processes, and yield for different generations of biodiesel. *Fuel* **2020**, *262*, 116553. [[CrossRef](#)]
41. Tubino, M.; Junior, J.G.R.; Bauerfeldt, G.F. Biodiesel synthesis: A study of the triglyceride methanolysis reaction with alkaline catalysts. *Catal. Commun.* **2016**, *75*, 6–12. [[CrossRef](#)]
42. Kwon, E.E.; Kim, S.; Jeon, Y.J.; Yi, H. Biodiesel Production from Sewage Sludge: New Paradigm for Mining Energy from Municipal Hazardous Material. *Environ. Sci. Technol.* **2012**, *46*, 10222–10228. [[CrossRef](#)]
43. Mondala, A.; Liang, K.; Toghiani, H.; Hernandez, R.; French, T. Biodiesel production by in situ transesterification of municipal primary and secondary sludges. *Bioresour. Technol.* **2009**, *100*, 1203–1210. [[CrossRef](#)]
44. Pastore, C.; Lopez, A.; Mascolo, G. Efficient conversion of brown grease produced by municipal wastewater treatment plant into biofuel using aluminium chloride hexahydrate under very mild conditions. *Bioresour. Technol.* **2014**, *155*, 91–97. [[CrossRef](#)]
45. Pastore, C.; Barca, E.; Del Moro, G.; Lopez, A.; Mininni, G.; Mascolo, G. Recoverable and reusable aluminium solvated species used as a homogeneous catalyst for biodiesel production from brown grease. *Appl. Catal. A Gen.* **2015**, *501*, 48–55. [[CrossRef](#)]
46. Matsumura, S. Enzyme-Catalyzed Synthesis and Chemical Recycling of Polyesters. *Macromol. Biosci.* **2002**, *2*, 105–126. [[CrossRef](#)]
47. Ajith, B.; Math, M.; Gc, M.P.; Parappagoudar, M.B. Analysis and optimisation of transesterification parameters for high-yield *Garcinia Gummi-Gutta* biodiesel using RSM and TLBO. *Aust. J. Mech. Eng.* **2020**, 1–16. [[CrossRef](#)]

48. Ferella, F.; Di Celso, G.M.; De Michelis, I.; Stanisci, V.; Vegliò, F. Optimization of the transesterification reaction in biodiesel production. *Fuel* **2010**, *89*, 36–42. [[CrossRef](#)]
49. Kansedo, J.; Lee, K.T.; Bhatia, S. Biodiesel production from palm oil via heterogeneous transesterification. *Biomass Bioenergy* **2009**, *33*, 271–276. [[CrossRef](#)]
50. Silva, G.F.; Camargo, F.L.; Ferreira, A.L. Application of response surface methodology for optimization of biodiesel production by transesterification of soybean oil with ethanol. *Fuel Process. Technol.* **2011**, *92*, 407–413. [[CrossRef](#)]
51. Demirbas, A. Biofuels sources, biofuel policy, biofuel economy and global biofuel projections. *Energy Convers. Manag.* **2008**, *49*, 2106–2116. [[CrossRef](#)]
52. Escobar, J.C.; Lora, E.S.; Venturini, O.J.; Yáñez, E.E.; Castillo, E.F.; Almazan, O. Biofuels: Environment, technology and food security. *Renew. Sustain. Energy Rev.* **2009**, *13*, 1275–1287. [[CrossRef](#)]
53. Wang, Y.; Feng, S.; Bai, X.; Zhao, J.; Xia, S. Scum sludge as a potential feedstock for biodiesel production from wastewater treatment plants. *Waste Manag.* **2016**, *47*, 91–97. [[CrossRef](#)]
54. Kargbo, D.M. Biodiesel Production from Municipal Sewage Sludges. *Energy Fuels* **2010**, *24*, 2791–2794. [[CrossRef](#)]
55. Bi, C.-H.; Min, M.; Nie, Y.; Xie, Q.-L.; Lu, Q.; Deng, X.-Y.; Anderson, E.; Li, N.; Chen, P.; Ruan, R. Process development for scum to biodiesel conversion. *Bioresour. Technol.* **2015**, *185*, 185–193. [[CrossRef](#)] [[PubMed](#)]
56. Capodaglio, A.G.; Callegari, A. Feedstock and process influence on biodiesel produced from waste sewage sludge. *J. Environ. Manag.* **2018**, *216*, 176–182. [[CrossRef](#)] [[PubMed](#)]
57. Olkiewicz, M.; Torres, C.M.; Jiménez, L.; Font, J.; Bengoa, C. Scale-up and economic analysis of biodiesel production from municipal primary sewage sludge. *Bioresour. Technol.* **2016**, *214*, 122–131. [[CrossRef](#)]
58. Silva, J.F.L.; Grekin, R.; Mariano, A.P.; Filho, R.M. Making Levulinic Acid and Ethyl Levulinate Economically Viable: A Worldwide Technoeconomic and Environmental Assessment of Possible Routes. *Energy Technol.* **2018**, *6*, 613–639. [[CrossRef](#)]
59. Serra, S.; De Simeis, D. New insights on the baker's yeast-mediated hydration of oleic acid: The bacterial contaminants of yeast are responsible for the stereoselective formation of (R)-10-hydroxystearic acid. *J. Appl. Microbiol.* **2018**, *124*, 719–729. [[CrossRef](#)] [[PubMed](#)]
60. Schwiderski, M.; Kruse, A. Process design and economics of an aluminium chloride catalysed organosolv process. *Biomass Convers. Biorefinery* **2016**, *6*, 335–345. [[CrossRef](#)]
61. Fulmer, G.R.; Miller, A.J.M.; Sherden, N.H.; Gottlieb, H.E.; Nudelman, A.; Stoltz, B.M.; Bercaw, J.E.; Goldberg, K.I. NMR Chemical Shifts of Trace Impurities: Common Laboratory Solvents, Organics, and Gases in Deuterated Solvents Relevant to the Organometallic Chemist. *Organometallics* **2010**, *29*, 2176–2179. [[CrossRef](#)]
62. Pastore, C.; D'Ambrosio, V. Intensification of Processes for the Production of Ethyl Levulinate Using $\text{AlCl}_3 \cdot 6\text{H}_2\text{O}$. *Energies* **2021**, *14*, 1273. [[CrossRef](#)]